

## **‘Internal’ and ‘external’ vibrational modes of CO<sub>2</sub>/NaCl(001) studied by Fourier-transform infrared spectroscopy and helium atom scattering**

J. Heidberg<sup>a</sup>, E. Kampshoff<sup>a</sup>, R. Kühnemuth<sup>a</sup> and O. Schönekas<sup>a</sup>  
G. Lange<sup>b</sup>, D. Schmicker<sup>b</sup>, J.P. Toennies<sup>b</sup>, R. Vollmer<sup>b</sup> and H. Weiss<sup>a,b</sup>

<sup>a</sup> Institut für Physikalische Chemie und Elektrochemie der Universität Hannover, Callinstr. 3-3a, 30167 Hannover, Germany

<sup>b</sup> Max-Planck-Institut für Strömungsforschung, Bunsenstr. 10, 37073 Göttingen, Germany

Employing two non-destructive methods, Fourier-transform infrared spectroscopy (FTIRS) and helium atom scattering (HAS), the adsorbate CO<sub>2</sub>/NaCl(001) was investigated in the frequency range from <10 cm<sup>-1</sup> to 5000 cm<sup>-1</sup>. The ‘internal’ vibrations  $\nu_2$ ,  $\nu_3$ ,  $\nu_3+2\nu_2$  and  $\nu_3+\nu_1$  were studied using FTIRS. The  $\nu_2$  and  $\nu_3$  are split due to a correlation field between two molecules in each adsorbate unit cell. In addition the degeneracy of the  $\nu_2$  bending vibrations is lifted on the surface, yielding a quartet absorption. Outside the experimental resolution the combination vibrations  $\nu_3+2\nu_2$  and  $\nu_3+\nu_1$  are not split, as expected from their low absorption cross section. The temperature dependence of the  $\nu_3$  doublet is explained in terms of small changes of the adsorption geometry, possibly due to the excitation of adsorbate phonons (‘external’ modes, i.e. vibrations of the molecules in the adsorption potential). In HAS experiments these phonons were studied. Below 80 cm<sup>-1</sup> a total of eight different modes was observed, some of which could be followed across the whole Brillouin zone. Above 80 cm<sup>-1</sup> several overtone/multiphonon excitations were also observed.

### **1. INTRODUCTION**

Vibrational spectroscopy is one of the most important tools for the study of adsorbates [1]. This is particularly true for adsorption on single crystal insulator substrates, where the often used electron spectroscopies can cause surface charging and surface damage. In recent years it has been demonstrated how orientational, structural, thermodynamic and dynamic data can be obtained for these physisorption systems if infrared spectra are recorded as a function of sample temperature, gas pressure and polarization of the infrared light. Observed were well-ordered adsorbate layers, domains containing 10<sup>4</sup> or more molecules, two-dimensional gas-solid as well as orientational phase transitions, and more. Since the perturbation of the molecules due to the coupling to the surface is weak, and the intramolecular forces are of similar

magnitude as the adsorption forces, these adsorbates may be viewed as two-dimensional molecular crystals. Systems studied so far include, e.g., CO<sub>2</sub> [2-9], CO [10-12], and CH<sub>4</sub> [13] on NaCl(001) and MgO(001) single crystal surfaces.

The present paper shall give an account of the present state of vibrational spectroscopy in the adsorbate CO<sub>2</sub>/NaCl(001). This adsorbate is, next to CO/NaCl(001), the best-studied system on well-defined insulator surfaces. Previously published were investigations of the  $\nu_2$  bending vibrations and the  $\nu_3$  asymmetric stretching vibration. From their observation orientational, structural and thermodynamic data were deduced. Here for the very first time spectra of the combination vibration  $\nu_3+\nu_1$  are presented. In combination with preliminary results on the combination vibration  $\nu_3+2\nu_2$  they allow to conclude on the Fermi splitting. The five expected ‘external’ modes - vibrations of CO<sub>2</sub> molecules in

the adsorption potential - are to low in frequency as to be easily detectable with infrared spectroscopy. Inelastic helium atom scattering is the appropriate non-destructive method for the observation of these modes. It allows not only to measure their frequencies but also their dispersion, thus providing the most direct information on the coupling of the molecules to the substrate and to each other. By employing these non-destructive companion methods - Fourier-transform infrared spectroscopy (FTIRS) and helium atom scattering (HAS) - the frequency range from  $< 10 \text{ cm}^{-1}$  to about  $5000 \text{ cm}^{-1}$  could be studied, allowing to draw an as complete as possible picture of the vibrational properties of the adsorbate  $\text{CO}_2/\text{NaCl}(001)$ .

## 2. EXPERIMENTAL

The experimental setups for adsorbate infrared spectroscopy [3] and helium atom scattering [14] are discussed in detail elsewhere. Here the major features will be described only. In the infrared experiment a uhv chamber is flanged to an evacuable interferometer (Bruker IFS 113v) and - at the opposite side - to an evacuable detector compartment. The uhv chamber is equipped with indium-sealed KBr windows for the frequency range above  $200 \text{ cm}^{-1}$ . The infrared light is polarized with a wire-grid polarizer. Spectra are recorded in transmission geometry, the angle of incidence relative to the surface normal being  $50^\circ \pm 3^\circ$ . The maximum resolution is  $\approx 0.06 \text{ cm}^{-1}$  around  $2000 \text{ cm}^{-1}$  and  $\approx 0.03 \text{ cm}^{-1}$  around  $600 \text{ cm}^{-1}$ , as determined from gas phase spectra. Depending on the spectral range studied, an InSb or GeCu detector were used.

The helium atom scattering experiments were carried out in another uhv chamber. A highly monoenergetic atom beam with an energy spread  $\Delta E/E \approx 1\%$  is produced in a supersonic expansion. It passes several beam-defining apertures and a variable speed, variable pulse width chopper before impinging onto the sample surface. The angle between incoming and outgoing beam is fixed at  $90^\circ$ . Scattered atoms are detected by a differentially pumped mass spectrometer located at the end of a flight tube. The energy transfer between the helium atoms and the surface is determined from measured

time-of-flight (TOF) spectra. Different momentum transfers  $\Delta K$  parallel to the surface are probed by sample rotation around an axis normal to the scattering plane (polar rotation). The energy resolution in the experiments reported herein is  $\approx 3 \text{ cm}^{-1}$  (0.35 meV) at  $112 \text{ cm}^{-1}$  (14 meV) beam energy, as determined from elastically scattered atoms.

In both experimental setups high-quality  $\text{NaCl}(001)$  single crystal planes were prepared under uhv conditions by in situ cleavage after bakeout. Sharp helium atom diffraction features and selective adsorption/desorption processes were observed on the bare substrate. They are indicative of clean surfaces which are atomically flat on a scale of at least a few thousand  $\text{NaCl}$  ion pairs.

Special care was taken to prepare the  $\text{CO}_2/\text{NaCl}(001)$  monolayer adsorbate under reproducible conditions. The samples were exposed to  $1\text{-}2 \cdot 10^{-8}$  mbar  $\text{CO}_2$  at  $T_{\text{sample}} \approx 80 \text{ K}$ . Infrared spectra taken under these conditions show the sharp doublet feature of the  $\nu_3$  doublet and no indication for growth of three-dimensional solid. In the scattering experiment the specular intensity of the helium atom beam drops continuously before reaching a constant value. The corresponding coverage is attributed to the monolayer. At the given sample temperature  $T_{\text{sample}} \approx 80 \text{ K}$  the gas flow can be stopped without noticeable desorption.

## 3. RESULTS AND DISCUSSION

Before presenting the vibrational spectra of  $\text{CO}_2/\text{NaCl}(001)$  we will briefly summarize the available structural information which is based on infrared spectroscopy, diffraction, and theory. From infrared spectroscopy it was inferred that the  $\text{CO}_2$  molecular axis is tilted by  $\approx 37^\circ$  relative to the surface plane, and that at least two molecules adsorb in each adsorbate lattice unit cell on energetically equivalent sites [2-6]. This conclusion is supported by a LEED study of  $\text{CO}_2$  on  $\text{NaCl}(001)$  films grown epitaxially on  $\text{Ge}(001)$ : a commensurate  $(2 \times 1)$  superstructure of  $pg$  symmetry was found in which two molecules in a unit cell are related via a glide plane [9]. Our own helium atom diffraction patterns are in agreement with the LEED study. We therefore regard the differences to another HAS

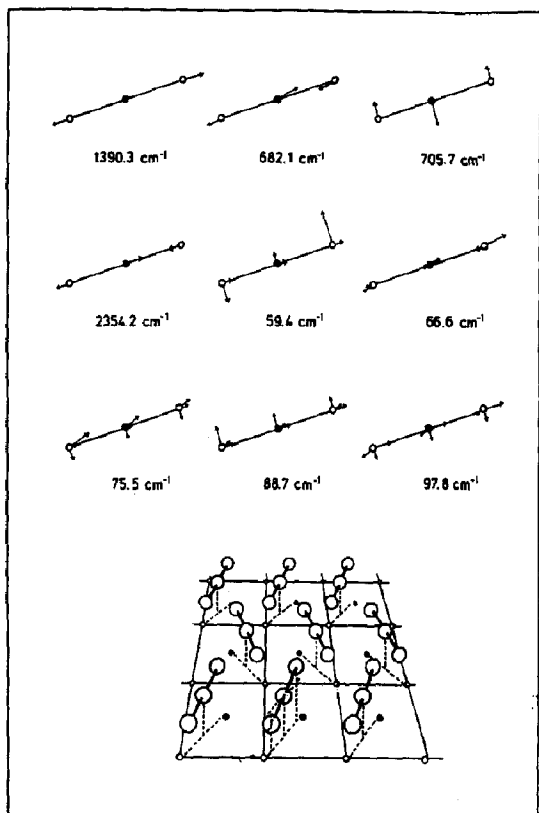


Figure 1. Calculated normal modes and structure of the monolayer  $\text{CO}_2/\text{NaCl}(001)$ . The mode labeling  $Q_1$ - $Q_9$  used in the text is from the left to the right and from the top to the bottom (adapted from reference [15]).

investigation [8], in which a more complex unit cell is suggested, as due to different conditions of monolayer preparation.

In a theoretical study Heidberg et al. developed a potential which reproduced the experimental adsorption energy, the molecular orientation and the  $(2 \times 1)$  adsorbate symmetry [15]. The two molecules in each unit cell enclose an angle of  $\approx 80^\circ$ , and a herringbone-like pattern is formed (see Fig. 1, bottom). Based on this reliable potential the normal vibrations of  $\text{CO}_2$  molecules in the monolayer were calculated under the constraint of identical displacements of the two molecules in each unit cell. A total of four 'internal' ( $Q_1$ - $Q_4$ ) and five 'external' ( $Q_5$ - $Q_9$ ) modes results. These modes are sketched in

Figure 1 (top). Mode  $Q_1$  corresponds to the symmetric stretch  $\nu_1$ ,  $Q_2$  and  $Q_3$  to the bending vibration  $\nu_2$ , which is twofold degenerate in the gas phase, and  $Q_4$  to the asymmetric stretch vibration  $\nu_3$ . It is noteworthy that a site symmetry splitting of the  $\nu_2$  bending vibration on the surface is predicted. Each of the 'external' modes  $Q_5$ - $Q_9$  contains translational as well as rotational components of the whole molecule on the surface.

Removing the constraint of identical displacements would result in a splitting of each of these modes in an in-phase and an out-of-phase vibration.

### 3.1. The 'internal' vibrations

Due to its superior resolution and the sensitivity of modern infrared detectors FTIR-spectroscopy is the method of choice to study the internal vibrations of  $\text{CO}_2$  at  $\text{NaCl}(001)$ . In the highly ordered  $(2 \times 1)$  structure a long-range order correlation field is formed resulting in principle in a splitting of all modes in a in-phase and out-of-phase vibration [2-4,16]. At 80 K the asymmetric  $\nu_3$  stretching vibration shows a doublet absorption at  $2349.1 \text{ cm}^{-1}$  and  $2339.9 \text{ cm}^{-1}$  (Fig. 2, middle). Upon isotopic dilution the doublet absorptions merge and yield a single absorption at  $\approx 2349 \text{ cm}^{-1}$ , the frequency of a vibrationally decoupled molecule. The influence of parameters like tilt angle, azimuthal angle of the molecules on the surface and isotopic composition of the adsorbate on the line shape and peak frequency of this doublet has been calculated using equations of classical electrodynamics for the description of the dipole-dipole coupling [3,16,17].

The  $\nu_2$  bending vibration of the monolayer  $\text{CO}_2$ - $\text{NaCl}(001)$  was also detected. As predicted by the normal coordinate analysis, its twofold degeneracy in the gas phase is lifted under the influence of the surface (site symmetry splitting) [4,15]. In the correlation field finally a quartet absorption at  $663.2 \text{ cm}^{-1}$ ,  $659.3 \text{ cm}^{-1}$ ,  $655.8 \text{ cm}^{-1}$  and  $652.8 \text{ cm}^{-1}$  results (Figure 2, right). Based on isotope dilution experiments the magnitude of the site symmetry splitting was determined to  $\approx 4.5 \text{ cm}^{-1}$  [17]. In this limit of dipole-decoupled molecules the  $\nu_2$  vibration 'parallel' to the surface ( $Q_2$  in Figure 1) absorbs at  $660 \text{ cm}^{-1}$ , the 'perpendicular' vibration ( $Q_3$ ) at  $655.5 \text{ cm}^{-1}$  as determined from their polarization dependence. In the experiment the energetic order of

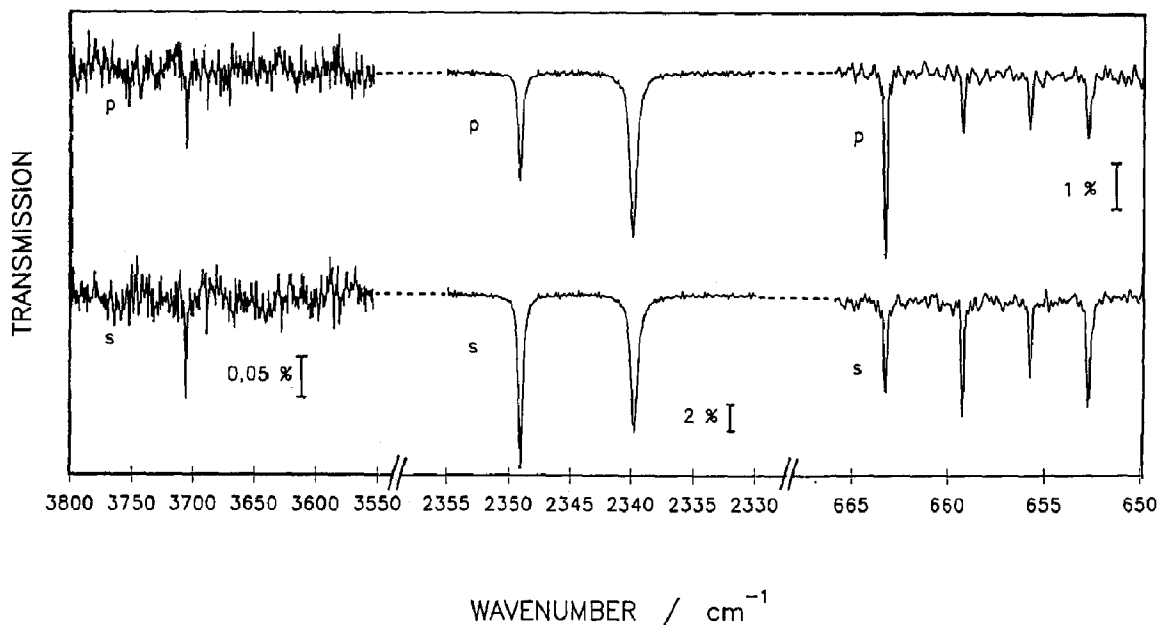


Figure 2. Polarized infrared transmission spectra of a monolayer  $^{12}\text{C}^{16}\text{O}_2$  on the NaCl(001) cleavage plane at 80 K. Angle of incidence  $50^\circ \pm 3^\circ$ , s- and p-polarization.

- left: combination vibration  $\nu_3 + \nu_1$ .  $\text{CO}_2$  pressure  $2 \cdot 10^{-8}$  mbar, InSb detector, instrumental resolution  $0.5 \text{ cm}^{-1}$ .
- middle: asymmetric stretching vibration  $\nu_3$ .  $\text{CO}_2$  pressure  $1 \cdot 10^{-8}$  mbar, GeCu detector, instrumental resolution  $0.2 \text{ cm}^{-1}$ .
- right: bending vibration  $\nu_2$ .  $\text{CO}_2$  pressure  $1 \cdot 10^{-8}$  mbar, GeCu detector, instrumental resolution  $0.2 \text{ cm}^{-1}$ .

these two vibrations is swapped as compared to theory.

The symmetric  $\nu_1$  stretching vibration, being only Raman active in the gas phase, should become IR active in the adsorbate. In  $\text{CO}_2$  adsorbates on evaporated NaCl films the  $\nu_1$  had been observed with peak intensities being smaller by a factor of 1000 in comparison with the corresponding  $\nu_3$  absorption [18]. Assuming the same factor for  $\text{CO}_2$  adsorbates on NaCl(001) cleavage planes  $\nu_1$  peak absorptions of about 0.01 % are expected. Absorptions that small are not yet detectable due to the signal-to-noise ratio of the interferometer. An indirect proof of the  $\nu_1$  is possible by means of combination vibrations, which have been observed in adsorbed  $\text{CO}_2/\text{NaCl}(001)$  for the first time. These vibrations are difficult to measure due to the poor signal-to-noise ratio and

spurious absorptions in the spectral range above  $3000 \text{ cm}^{-1}$ . A single absorption at  $3705.5 \text{ cm}^{-1}$  (Figure 2, left) is attributed to the combination mode  $\nu_3 + \nu_1$ . Using attenuated total reflection (ATR) spectroscopy another single absorption at  $3597.9 \text{ cm}^{-1}$  has been detected recently. This absorption, which is not shown in Figure 2, is attributed to  $\nu_3 + 2\nu_2$ . A doublet splitting of the combination vibrations is not detected. However, this result is not in contradiction to the correlation field in the unit cell. The splitting  $\Delta\nu$  of a vibration in a correlation field depends strongly on its vibrational polarizability  $\alpha_v$  [19]. The dependency is described in eq. (1), where  $\alpha_e$  is the electronic polarizability and U is the lattice sum of the adsorbate:

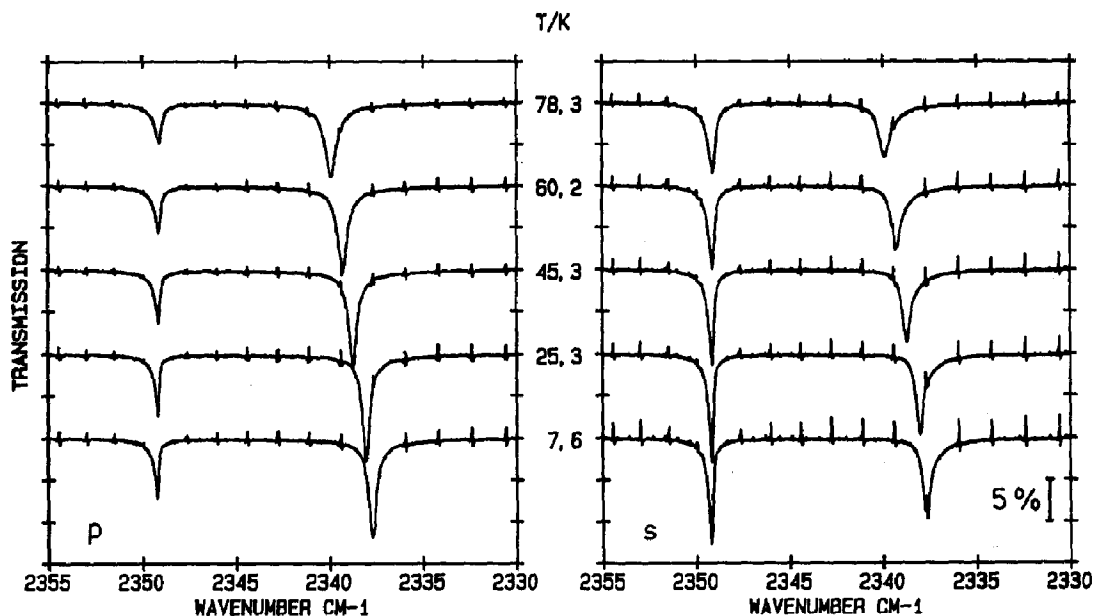


Figure 3. Temperature dependence of the p- and s-polarized  $\nu_3$  transmission spectra of a monolayer  $^{12}\text{C}^{16}\text{O}_2$  on the NaCl(100) cleavage plane (from reference [6]).

$$\nu^\pm = \nu_0 \cdot \sqrt{1 + \frac{\alpha_v \cdot U^\pm}{1 + \alpha_e \cdot U^\pm}} \quad (1)$$

$$\Delta\nu^\pm = |\nu^+ - \nu^-|$$

$$\approx \nu_0 \cdot \sqrt{\alpha_v} \cdot \left( \sqrt{\frac{U^+}{1 + \alpha_e U^+}} + \sqrt{\frac{U^-}{1 + \alpha_e U^-}} \right)$$

The in-phase and out-of-phase vibrations are denoted by + and -, respectively. Their frequency splitting  $\Delta\nu^\pm$  depends on  $\alpha_v^{1/2}$ . The vibrational polarizability  $\alpha_v$  itself is linearly related to the absorption cross section. Therefore weak absorptions like the combination vibrations or the  $\nu_1$  mode are expected to show only a very small splitting, which is probably not resolved in the absorption spectra.

In the gas phase of  $\text{CO}_2$  the  $\nu_1$  and the first overtone of the bending vibration  $2\nu_2$  are in Fermi resonance yielding a doublet separated by about  $103 \text{ cm}^{-1}$ , while the combination vibrations  $\nu_3 + \nu_1$  and  $\nu_3 + 2\nu_2$  are separated by  $107 \text{ cm}^{-1}$  [20]. This value

is almost identical to that reported herein ( $\approx 108 \text{ cm}^{-1}$ ), in agreement with an only weak perturbation of the molecules due to the surface.

The external vibrations of the monolayer  $\text{CO}_2/\text{NaCl}(001)$ , which are expected below  $100 \text{ cm}^{-1}$  [15], are not detectable by means of FTIR-spectroscopy. Nevertheless they influence the frequency and full width at half maximum (FWHM) of the internal absorptions by a vibrational phase relaxation process [21]. As a result of this influence the  $\nu_3$  absorption spectra of the monolayer  $\text{CO}_2/\text{NaCl}(001)$  strongly depend on the substrate temperature (Fig. 3). Using the exchange model to describe the vibrational phase relaxation [21], the temperature-dependency of frequency and FWHM of the  $\nu_3$  absorption spectra has been calculated in agreement with the experimental results [6]. Three 'external' vibrations at  $\approx 29 \text{ cm}^{-1}$ ,  $\approx 48 \text{ cm}^{-1}$  and  $\approx 60 \text{ cm}^{-1}$  were taken into account in these calculations. These frequencies were provided by HAS experiments which will be described below. Although the frequency shift upon temperature decrease is significant, it is accompanied by small changes of

less than 2% in the structural parameters - molecular tilt angle and azimuthal angle - only.

In contrast to the  $\nu_3$  doublet the  $\nu_2$  quartet peak frequencies are only slightly temperature dependent.

### 3.2. The 'external' vibrations

The theoretical study by Heidberg et al. placed the frequencies of the 'external' vibrations in the range below  $100 \text{ cm}^{-1}$ , a domain of HAS experiments [15]. Preliminary experiments with a beam energy  $E_i=33 \text{ meV}$  confined the fundamental modes to below  $\approx 80 \text{ cm}^{-1}$ . In order to obtain high resolution the TOF spectra presented herein were measured with  $14 \text{ meV}$  ( $112 \text{ cm}^{-1}$ ) incident beam energy, corresponding to a wave vector  $k_i=5.17 \text{ \AA}^{-1}$ . This wave vector is larger than the reciprocal lattice vector of the substrate ( $G=1.58 \text{ \AA}^{-1}$ ), thus allowing to transfer momentum between atoms and surface and to measure collective vibrations ('adsorbate phonons') across more than one Brillouin zone. In contrast to this, infrared phonons carry negligible momentum, and all unit cells are excited in-phase only ( $Q=0$  mode, where  $Q$  is the wave vector of the collective adlayer vibration parallel to the surface).

For the  $90^\circ$  fixed angle geometry between incoming and outgoing beam the momentum transfer  $\Delta K$  parallel to the surface and the energy loss or gain  $\Delta E$  of helium atoms scattered from the surface are related by the so-called 'scan curve'

$$\frac{\Delta E}{E_i} = \frac{\left[ \sin\theta_i + \frac{\Delta K}{k_i} \right]^2}{\cos^2\theta_i} - 1 \quad (2)$$

Thus for a given angle of incidence  $\theta_i$  relative to the surface normal a particular energy transfer  $\Delta E$  is strictly related to a momentum transfer  $\Delta K$ . In the present study TOF spectra were recorded in the  $\langle 110 \rangle$  azimuthal direction ( $\overline{1}\overline{1}X$  direction). The  $\theta_i$  range between  $43^\circ$  and  $57^\circ$  was probed in steps of  $0.5^\circ$ , allowing to follow modes across more than one Brillouin zone.

Figure 4 shows the spectra (transformed to an energy transfer scale) for incident angles  $\theta_i$  ranging from  $43^\circ$  to  $49^\circ$ . In order to suppress the inelastic multiphonon background the sample was cooled to

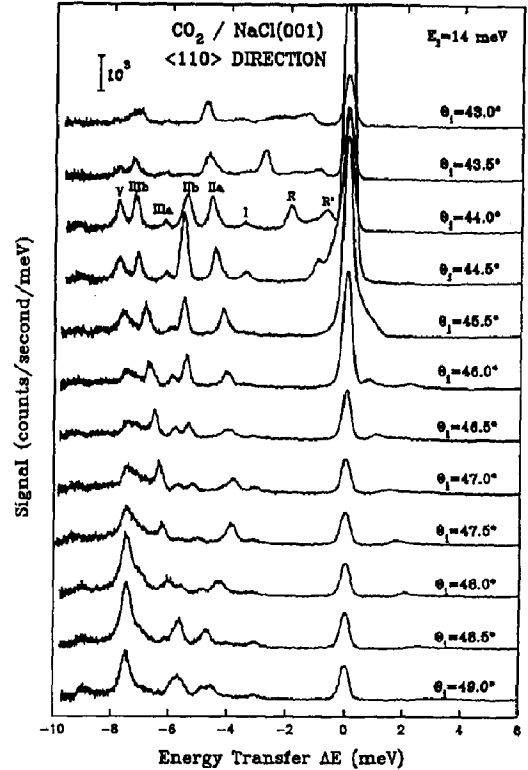


Figure 4. Energy transfer spectra of monolayer  $\text{CO}_2/\text{NaCl}(001)$  obtained from time-of-flight spectra at different angles of incidence.  $T_{\text{sample}}=30 \text{ K}$ ,  $\langle 110 \rangle$  azimuthal direction,  $E_i=14 \text{ meV}$ . For each spectrum  $3.6 \cdot 10^6$  signals were accumulated (chopper speed  $500 \text{ Hz}$ , chopper pulse width  $15 \mu\text{s}$ ). The phonon labels exemplary shown in the  $44^\circ$  spectrum are explained in the text.

$30 \text{ K}$ . No structural changes were observed upon cooling. At this low temperature mostly energy loss and only few gain features are observed, respectively. The peak at zero energy is due to helium atoms scattered inelastically from random defects on the surface. The parallel momentum transfer  $\Delta K$  of each energy loss or gain feature can be calculated using eq. (2). By subtracting the reciprocal lattice vector  $G$  of the  $\text{NaCl}(001)$  substrate or a multiple of it, it can be transformed to the phonon wave vector  $Q$  (we use the term

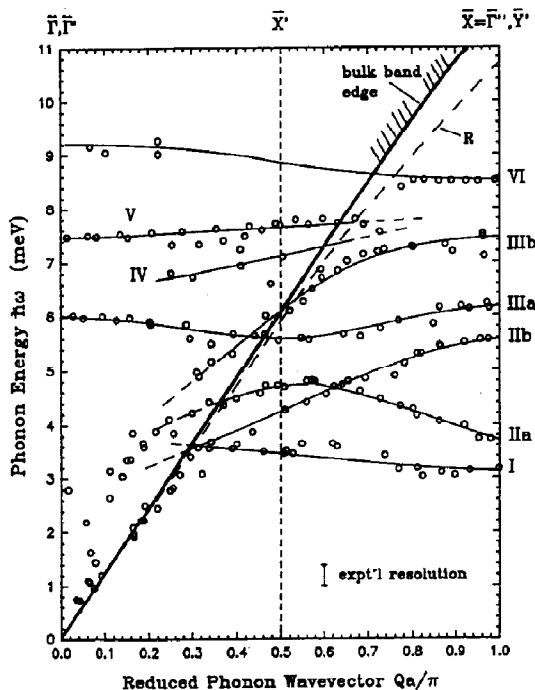


Figure 5. Phonon dispersion curves of the monolayer  $\text{CO}_2/\text{NaCl}(001)$ ,  $\langle 110 \rangle$  azimuthal direction.  $a=3.96 \text{ \AA}$ .  $E_i=14 \text{ meV}$ ,  $k_i=5.17 \text{ \AA}^{-1}$ . The phonon branch labeling is explained in the text [22].

'phonon' for the collective 'external' vibrations of the  $\text{CO}_2$  molecules in the monolayer). The resulting pairs  $(\hbar\omega, Q)$ , where  $\hbar\omega=|\Delta E|$  is the phonon energy, are plotted in Figure 5 [22]. The data points are assigned to discrete modes by the solid lines which were drawn in by eye. This preliminary assignment is by no means unique. None of these modes were observed on the bare  $\text{NaCl}(001)$  substrate.

In order to discuss the phonon modes, knowledge of the Brillouin zones of  $\text{NaCl}(001)$  and the monolayer  $\text{CO}_2/\text{NaCl}(001)$  is necessary [23]. They are shown in Figure 6. Due to the  $(2 \times 1)$  superstructure of the  $\text{CO}_2$  monolayer its Brillouin zone is smaller than that of the bare  $\text{NaCl}$ . Two different types of domains exist, one with the glide

plane parallel to the  $\langle 110 \rangle$  direction and one which is rotated by  $90^\circ$ , having the glide plane in the  $\langle \bar{1}\bar{1}0 \rangle$  direction (for a pictorial representation compare Figure 1, bottom). Both types of domains will always be present in our experiment, and the TOF spectra in Figure 3 represent a superposition of modes along the  $\Delta'$  and the  $\Sigma'$  direction.

With two molecules per unit cell each of the five 'external' modes of a single  $\text{CO}_2$  molecule splits into two and therefore ten phonon modes are to be expected for the  $\Delta'$  as well as for the  $\Sigma'$  direction. However, for the  $\Delta'$  direction selection rules apply: (i) The split modes are of even and odd symmetry, respectively, and are necessarily degenerate at the zone boundary  $\bar{X}'$  [24]. (ii) For symmetry reasons even modes can be observed in the first, third ... Brillouin zone, while odd modes can be observed in the second, fourth ... zone only [25]. Taking into account these constraints, the maximum number of modes observable at a given  $\Delta K$  is 15. We note however that not all these modes must be split in energy, and since the interaction of the helium atoms is largest for modes which have a large

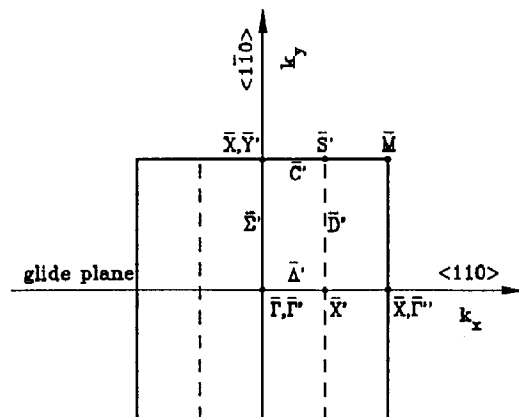


Figure 6. Surface Brillouin zone of  $\text{NaCl}(001)$  (solid lines) and the Brillouin zone of the  $\text{CO}_2$  monolayer superstructure (dashed line). The  $\langle 110 \rangle$  and  $\langle \bar{1}\bar{1}0 \rangle$  directions correspond to the  $\text{NaCl}$  structure. Symbols denoting the superstructure Brillouin zone are marked by a prime ('). For a real space structure see Figure 1, bottom.

displacement perpendicular to the surface not all modes may be detected.

Based on these considerations we can discuss the phonons in Figure 5. A total of eight modes is observed, well below the maximum number of 15. We number the modes with increasing energy at the zone boundary. Crossings are not expected for modes of same symmetry. They indicate that these modes either correspond to different directions or to different symmetry. Branches crossing each other are therefore labelled a and b, respectively.

The dashed curve in Figure 5 corresponds to the Rayleigh wave R of the bare NaCl(001) substrate, an acoustic wave which propagates parallel to the surface, decays exponentially with increasing depth into the crystal, and is polarized in the sagittal plane (the plane containing the surface normal and the direction of propagation). Other NaCl phonon modes exist for pairs of smaller  $Q$ , larger  $\hbar\omega$  than the Rayleigh wave only. Close to the zone boundary, and far away from substrate phonon regions, the influence of substrate-adlayer coupling is small, and modes in this range are located mainly in the topmost layer, i.e. in the CO<sub>2</sub> adlayer. In the bulk band region the vibrational modes of the CO<sub>2</sub> layer can mix with the bulk bands and become a resonance. A very strong coupling can cause broadening and damping because of energy leakage. This may be the case for most of the low-energy adsorbate modes which are significantly broadened and disappear at wavevectors smaller  $Q=0.2\pi/a$ . At the zone origin  $\Gamma$  only the modes IIIa and V are clearly visible. Only mode IIIa can be followed easily across the entire Brillouin zone from  $\Gamma$  to X. This suggests small interference with NaCl modes. Mode V disappears soon after it passes the Rayleigh phonon. Around X' mode IIa has its highest intensity and modes IIIb, IV and V are clearly visible. At  $Q=\pi/a$ , which is the  $\Gamma'$  point for the one domain and also the zone boundary for the other, modes IIb, IIIb and IV are strongest out of a total of 6 modes.

In the experiments with a higher beam energy ( $E_i=33.5$  meV) only the modes I/IIa, IIIa and V can be uniquely identified (these data points are not drawn in order to avoid a congestion of Figure 5). Modes I and IIa are hardly separated due to the lower resolution, IIIa is visible in the bulk band region only, and V is apparently visible even at the

zone boundary  $\bar{X}$ . However, the latter is probably due to an unresolved transition from mode V to IIIb upon passing the Rayleigh mode. Within the experimental resolution the energy of these modes is independent of the wave vector  $Q$  and was determined to  $\approx 3.6$  meV,  $\approx 6$  meV and  $\approx 7.5$  meV, corresponding to  $\approx 29$  cm<sup>-1</sup>,  $\approx 48$  cm<sup>-1</sup> and  $\approx 60$  cm<sup>-1</sup>, respectively. These mode energies were used for the theoretical description of the temperature dependence of the  $\nu_3$  absorption spectra (see above). At higher energies weak modes are observed at  $\approx 11$  meV,  $\approx 14.8$  meV,  $\approx 18.5$  meV and  $\approx 20.4$  meV. Due to their intensities and energies we attribute them to overtone/multiphonon excitations, e.g. V+I/IIa, 2V, 2V+I/IIa and 3V, respectively.

Due to the complexity of the phonon dispersion diagram a detailed and sophisticated interpretation is impossible without the aid of a lattice dynamical calculation, which is not yet available. Other systems studied so far - mainly rare gas layers and CO on different substrates - can not be used for comparison. However, a tentative assignment is possible on the base of the above mentioned normal coordinate calculation by Heidberg et al. [15]. The frequencies of the five 'external' modes  $Q_5$ - $Q_9$ , shown in Figure 1, range from 59.4 to 97.8 cm<sup>-1</sup>, corresponding to 7.5 to 12.2 meV. Due to the use of the second derivative of the adsorption potential for the calculation of these frequencies the absolute values are to be interpreted with care, and are indeed larger as those observed in the experiment. However, the relative sequence is expected to be correct.

Our tentative assignment of normal vibrations to the measured dispersion curves is based on the particular sensitivity of adsorbate motions perpendicular to the surface. The calculated mode  $Q_8$  has the largest amplitude normal to the surface, its dominant character being that of a hindered translation. For both incident beam energies (14 meV, 33.5 meV) the mode V was the easiest to observe. Therefore we assign it to  $Q_8$ .

In the calculation a significant normal component was also found for the lowest-frequency mode  $Q_5$ , a hindered rotation. The experimental data do not allow to assign unambiguously a measured mode to  $Q_5$ : While at 14 meV incident beam energy mode IIa is more intense than mode I, the TOF spectra at



$E_1=33.5$  meV show very pronounced energy loss features below 4 meV, i.e. in the range of mode I (it has to be born in mind that at the higher beam energy the modes I and IIa are not well separated). For energetic reasons, and due to its apparent intensity increase, we tentatively assign mode I to  $Q_5$ .

For similar energetic reasons  $Q_9$ , a mode with a large vibrational amplitude in the direction of the molecular axis, might be assigned to VI. The other two calculated modes  $Q_6$  and  $Q_7$  cannot be uniquely identified.

Finally we will discuss the influence of dipolar coupling on number and dispersion on the 'external' modes. The observed splitting of the 'internal'  $\text{CO}_2$  vibrations  $\nu_2$  and  $\nu_3$  is quantitatively explained by a correlation field splitting due to dipole-dipole coupling between the two molecules in the unit cell of the (2x1) adsorbate structure. The magnitude of this splitting is  $9 \text{ cm}^{-1}$  ( $\approx 1.1$  meV) in case of  $\nu_3$  and depends strongly on the vibrational polarisability  $\alpha_v$  (compare eq. 1). For the 'external' modes  $\alpha_v$  is very small. A correlation field splitting much smaller than 1 meV is expected for them, probably unresolvable by present HAS machines. Therefore dipole-dipole coupling has no influence on the number of modes reported herein.

For the same reason the influence of dipolar coupling on the phonon dispersion is small. It is determined by  $\alpha_v$  as well as the  $Q$  dependence of the 'dipole sum'  $U$  over the real-space lattice of the adsorbed dipoles. A straightforward estimation of the dispersion for the very strong  $\nu_3$  infrared absorption yields a value comparable to the shift observed in the isotope dilution experiments, i.e. a shift of 1-2 meV upon change of  $Q$  from  $\Gamma$  to  $X$ . Again the value for the 'external' modes is much less than 1 meV. The pronounced dispersion of the experimental modes IIb and IIIb can not be explained by dipolar coupling and must have another origin, like direct orbital interactions. It suggests that in the respective modes the dominant molecular motions are parallel, not perpendicular to the surface.

#### 4. SUMMARY AND CONCLUSIONS

Two non-destructive methods - Fourier-transform infrared spectroscopy with polarized light and helium atom scattering - were employed to elucidate the vibrational properties of the monolayer  $\text{CO}_2$  adsorbed on  $\text{NaCl}(001)$  single crystal planes, making it probably the best-studied system to date. The spectral range from  $5000 \text{ cm}^{-1}$  to  $<10 \text{ cm}^{-1}$  was investigated. The 'internal' vibrations - vibrations within the molecules -  $\nu_2$  and  $\nu_3$  are split due to a correlation field between two molecules in a unit cell of the adsorbate lattice. In addition, the  $\nu_2$  is split due to the site symmetry which lifts the degeneracy. As expected, no splitting is observed for the weakly infrared active combination vibrations  $\nu_3 + 2\nu_2$  and  $\nu_3 + \nu_1$  which are reported for the first time. They are separated by  $\approx 108 \text{ cm}^{-1}$ , partially due to the Fermi resonance. This value is comparable to the gas phase value. The 'external' vibrations or 'adsorbate phonons', i.e. collective periodic motions of the molecules in the adsorption potential, were studied by high-resolution inelastic helium atom scattering. They can influence the peak position, lineshape and linewidth of the 'internal' vibrations. Based on symmetry considerations up to 15 different modes are expected. The phonon dispersion diagram shows eight different modes below  $80 \text{ cm}^{-1}$ . The complexity of the diagram does not allow a complete interpretation without the aid of a lattice dynamical computation which is in progress [26]. However, a tentative identification of two of these modes is possible based on a previous normal coordinate calculation at the zone origin. Due to their strong dispersion two other modes are assigned to in-plane vibrations with significant short-range interactions.

The present paper should serve not only to draw a complete-as-possible picture of the vibrational properties of the monolayer  $\text{CO}_2/\text{NaCl}(001)$  but also to demonstrate the complexity and richness of phenomena in well-defined adsorbates on insulator surfaces. Other systems studied in close cooperation between our groups in Hannover and Göttingen include  $\text{CO}/\text{NaCl}(001)$  and  $\text{CH}_4/\text{NaCl}(001)$ . The phenomena observed so far are no less fascinating than those observed for  $\text{CO}_2/\text{NaCl}(001)$ .

## ACKNOWLEDGEMENTS

We thank the Deutsche Forschungsgemeinschaft (DFG), the Fonds der Chemischen Industrie (FCI) and the Land Niedersachsen for financial support. One of us (H.W.) thanks the DFG and the FCI for scholarships.

## REFERENCES

1. For a review see: Y.J. Chabal, *Surf. Sci. Rep.* 8 (1988) 211.
2. O. Berg and G.E. Ewing, *Surf. Sci.* 220 (1989) 207.
3. J. Heidberg, E. Kampshoff, O. Schönekas, H. Stein and H. Weiss, *Ber. Bunsenges. Phys. Chem.* 94 (1990) 112,118,127.
4. J. Heidberg, E. Kampshoff, R.Kühnemuth, O. Schönekas, H. Stein and H. Weiss, *Surf. Sci.* 226 (1990) L43.
5. O. Berg, R. Disselkamp and G.E. Ewing, *Surf. Sci.* 272 (1992) 8.
6. J. Heidberg, E. Kampshoff, R. Kühnemuth and O. Schönekas, *Surf. Sci.* 269/270 (1992) 120.
7. J. Heidberg and D. Meine, *Surf. Sci.* 279 (1992) L175; J. Heidberg and D. Meine, *Ber. Bunsenges. Phys. Chem.* 97 (1993) 211.
8. G.-Y. Liu, G.N. Robinson, G. Scoles and P.A. Heiney, *Surf. Sci.* 262 (1992) 409.
9. J. Schimmelpfennig, S. Fölsch and M. Henzler, *Surf. Sci.* 250 (1991) 198.
10. H.H. Richardson and G.E. Ewing, *J. Phys. Chem.* 91 (1987) 5833; G.E. Ewing, *Acc. Chem. Res.* 25 (1992) 292, and references therein.
11. J. Heidberg, K.W. Stahmer, H. Stein and H. Weiss, *J. Electron Spectrosc. Relat. Phenom.* 45 (1987) 87; J. Heidberg, E. Kampshoff, R. Kühnemuth, O. Schönekas and M. Suhren, *J. Electron Spectrosc. Relat. Phenom.* 54/55 (1990) 945; J. Heidberg, E. Kampshoff and M. Suhren, *J. Chem. Phys.* 95 (1991) 9408, and references therein.
12. D. Schmicker, J.P. Toennies, R. Vollmer and H. Weiss, *J. Chem. Phys.* 95 (1991) 9412.
13. O. Berg, L. Quattrocci, S.K. Dunn and G.E. Ewing, *J. Electron Spectrosc. Relat. Phenom.* 54/55 (1990) 981; L. Quattrocci and G.E. Ewing, *J. Chem. Phys.* 96 (1992) 4205.
14. G. Brusdeylins, R.B. Doak and J.P. Toennies, *Phys. Rev. B* 27 (1983) 3662; J.P. Toennies and R. Vollmer, *Phys. Rev. B* 44 (1991) 9833.
15. J. Heidberg, E. Kampshoff, R. Kühnemuth and O. Schönekas, *Surf. Sci.* 251/252 (1991) 314.
16. W. Chen and W.L. Schaich, *Surf. Sci.* 220 (1989) L733.
17. J. Heidberg, E. Kampshoff and R. Kühnemuth, to be published.
18. J. Heidberg, S. Zehme, C.F. Chen and H. Hartmann, *Ber. Bunsenges. Phys. Chem.* 75 (1971) 1009.
19. G.D. Mahan and A.A. Lucas, *J. Chem. Phys.* 68 (1978) 1344.
20. G. Herzberg, *Molecular Spectra and Molecular Structure Vol. II.*, Krieger, Malabar, 1991.
21. W. Erley and B.N.J. Person, *Surf. Sci.* 218 (1989) 494.
22. G. Lange, J.P. Toennies, R. Vollmer and H. Weiss, *J. Chem. Phys.* 98 (1993) 10096.
23. A.P. Cracknell, *Thin Solid Films* 21 (1974) 107.
24. F. Hund, *Z. Phys.* 99 (1936) 119.
25. K.C. Prince, *J. Electron Spectrosc. Relat. Phenom.* 42 (1987) 217.
26. G. Benedek and W. Vitali, 1993, private communication.